Free Energy Relationships in Metalloenzyme-Catalyzed Reactions. Calculations of the Effects of Metal Ion Substitutions in Staphylococcal Nuclease

Johan Åqvist[†] and Arieh Warshel*

Contribution from the Department of Chemistry, University of Southern California, Los Angeles, California 90089-1062. *Received June 12, 1989*

Abstract: Free energy perturbation calculations of the catalytic effects associated with substitutions of the active site Ca^{2+} ion in staphylococcal nuclease are reported. The calculated changes in the activation barrier for different ions are found to be consistent with kinetic measurements, and the catalytic rate of enzyme indeed appears to be optimized for Ca^{2+}. Our results indicate that the more electrophilic ions (with large hydration free energy) increase the activation barrier as a result of overstabilization of the intermediately created OH^- nucleophile and that the enzymatic rate is more affected by these ions than by those that are less electrophilic than Ca^{2+}. A simple model for treating transition-metal ions is also presented and calibrated for the Mn^{2+} ion in solution. The calculated decrease in activity when Mn^{2+} is bound to the enzyme agrees fairly well with experimental observations. Simple free energy relationships are outlined in order to classify different types of metal-catalyzed enzymatic reactions. These relationships demonstrate that the optimization of the catalytic effiency for a particular ion is related to its multiple tasks during the reaction; i.e., the ion must stabilize the negatively charged nuclephile as well as the subsequent transition state. Several other metalloenzymes are discussed in these terms, and it is argued that such free energy relationships can provide qualitative predictions of the effects associated with metal substitutions. Finally, a tentative qualitative classification of metalloenzymes is presented in terms of the interplay between metal and general-base catalysis, again based on linear free energy concepts.

The presence of active-site metal ions is a ubiquitous feature of enzymatic reactions, and these ions generally play a crucial role in the catalytic activity of the enzyme. In many cases the influence of a catalytic metal on the energetics of a given enzymatic reaction can be qualitatively well understood. However, more quantitative descriptions of how the metal acts in facilitating different reaction steps are not so easily obtained. The prerequisites for acquiring a deeper understanding of metalloenzyme-catalyzed reactions are now becoming available through an increasing amount of refined structural information, augmented by detailed kinetic data from site-specific mutation experiments. With this wealth of experimental data and recent progress in theoretical studies of enzyme reactions it is interesting to try to explore some of the questions concerning the special roles of catalytic metal ions and the reasons for the evolutionary selection of different meals in different cases. In particular, one would like to examine what general trends (if any) characterize metal ion assisted catalysis and how substitutions of the metal affect the catalytic action of a given enzyme. In the present paper, we examine these issues by calculating the effects of metal ion substitutions on the catalytic reaction of staphylococcal nuclease (SNase). It is well-known that enzymes that catalyze reactions involving the breakage and formation of phosphoric ester bonds often make use of divalent metal cations both for binding the negatively charged phosphate groups as well as for promoting nucleophilic displacements on the substrate (for reviews, see refs 1 and 2). The choices of catalytic ions, in these cases, include both alkaline-earth metals such as Ca^{2+} and Mg^{2+} as well as several transition metals. SNase provides an excellent test case for calculations in view of the availability of extensive kinetic information[3] and its sensitivity to replacement of the catalytic Ca^{2+} ion by other divalent cations.[3b,4] Furthermore, the mechanistic similarities between the SNase reaction and several other metalloenzyme-catalyzed reactions allow for interesting comparisons of the roles played by the metal ion in different cases.

We have previously reported a study[5] of the SNase reaction in which the empirical valence bond (EVB) scheme[6] was employed in combination with free energy perturbation (FEP) molecular dynamics (MD) simulations. The overall activation barrier for the enzyme was reproduced without any arbitrary adjustments of parameters, and calculations on the Asp 21 → Glu 21 mutation also yielded a change in the activation energy ($\Delta\Delta G^{\ddagger}_{cat}$) in good agreement with experimental data. These results corroborate the soundness of our modeling scheme for the SNase-catalyzed reaction and motivated us to use this system as a benchmark model for studying the role of metal ions in enzyme catalysis. This rather challenging problem is addressed by examining the sensitivity of the overall activation barrier, $\Delta G^{\ddagger}_{cat}$, to the size and hydration free energy of the active site metal ion, with FEP/MD calculations. Since the most reliable kinetic measurements on "ion mutants" involve replacement of Ca^{2+} by transition-metal ions, we also present a simple novel model for these ions. This model is implemented in the case of Mn^{2+} under the requirement that it should reproduce both the relevant radial distribution function as well as the observed hydration energy. The results from the present FEP/MD calculations agree fairly well with kinetic data, for both smaller and larger ions than Ca^{2+}, and it is demonstrated how the enzyme's active site appears to be designed to achieve a maximum turnover when Ca^{2+} is bound. Furthermore, the effect of replacing Ca^{2+} with less electrophilic ions, such as Sr^{2+}, is found to be less severe than is the case with smaller ions (with larger solvation energy in water).

The present study suggests a simple free energy relationship for the effect of catalytic metal ions in hydrolytic and related reactions. This relationship allows one to classify different reactions according to the apparent effect of metal substitution and to rationalize (and sometimes predict) the energy balance associated with the optimization for a particular ion. Both the present results as well as our earlier study emphasize the enormous catalytic effect associated with the presence of the metal ions, which appears to be a major factor in promoting the formation of the OH^- nucleophile from water, as well as for subsequent transition-state stabilization. The generality of this role played

[†] Present address: Department of Molecular Biology, Uppsala Biomedical Centre, Box 590 S-75124 Uppsala, Sweden.

(1) Mildvan, A. S. *Adv. Enzymol.* **1979**, *49*, 103-126.
(2) Knowles, J. R. *Ann. Rev. Biochem.* **1980**, *49*, 877-919.
(3) (a) Sepersu, E. H.; Shortle, D.; Mildvan, A. S. *Biochemistry* **1986**, *25*, 68-77. (b) Sepersu, E. H.; Shortle, D.; Mildvan, A. S. *Biochemistry* **1987**, *26*, 1289-1300. (c) Sepersu, E. H.; Hibler, D. W.; Gerlt, J. A.; Mildvan, A. S. *Biochemistry* **1989**, *28*, 1539-1548.
(4) Cuatrecasas, P.; Fuchs, S.; Anfinsen, C. B. *J. Biol. Chem.* **1967**, *242*, 1541-1547.
(5) Aqvist, J.; Warshel, A. *Biochemistry* **1989**, *28*, 4680-4689.
(6) (a) Warshel, A.; Weiss, R. M. *J. Am. Chem. Soc.* **1980**, *102*, 6218-6226. (b) Warshel, A.; Russell, S. T. *Q. Rev. Biophys.* **1984**, *17*, 283-422.

0002-7863/90/1512-2860$02.50/0

by the metal ion in a broad class of metalloenzyme reactions is pointed out.

Calculation Methods and Experimental Background

Staphylococcal nuclease is a well-characterized example of a phosphodiester-cleaving enzyme. A high-resolution crystal structure in complex with the inhibitor pdTp, which in some respects resembles the rate-limiting transition state, was determined by Cotton and co-workers[7a,b] and recently redetermined and refined by Loll and Lattman.[7c] In addition, several mutant versions of the enzyme have been studied by kinetic and spectroscopic techniques.[3,8] SNase requires one Ca^{2+} ion for its action and catalyzes the hydrolysis of both DNA and RNA at the 5′-position of the phosphodiester bond, yielding a free 5′-hydroxyl group and a 3′-phosphate monoester:[9]

$$H_2O + 5'\text{-}OP(O_2)^-O\text{-}3' \rightleftharpoons 5'\text{-}OH + (OH)P(O_2)^-O\text{-}3' \qquad (1)$$

A reaction mechanism for the enzyme was first postulated by Cotton et al.:[7b] (I) general-base catalysis by Glu 43, which abstracts a proton from a water molecule in the active site, yielding a free hydroxide ion; (II) nucleophile attack by the OH^- ion on the phosphorus atom in line with the 5′-O–P ester bond, leading to the formation of a trigonal-bipyramidal (i.e., pentacoordinated) transition state or metastable intermediate; (III) breakage of the 5′-O–P bond and formation of products. The catalytic rate constant for the wild-type enzyme is 95 s^{-1} at pH 7.5 and is limited by the second step above.[3a] In solution, this step is associated with an activation free energy barrier of about 33 kcal/mol.[10] The proposed reaction mechanism is strongly supported by kinetic studies of various mutants[3] as well as by recent free energy calculations by us.[5] However, both the study by Sepersu et al.[3b] and our previous calculations indicate that the active-site residue Arg 87 interacts primarily with the pentacoordinated transition state and not with the singly negatively charged phosphate group, as was originally suggested.[7b] As for step I, a recent study[3c] has shown that the Glu 43 → Ser 43 (E43S) mutant is 2700-fold less active than the native enzyme at pH 7.4, but only 370-fold at pH 9.9. This is clearly in accord with the role of Glu 43 as a general base. It is, however, interesting to note that the factor 2700 only accounts for only 5 kcal/mol of the cost of forming the OH^- nucleophile in water, which is about 21 kcal/mol. The quantitative effect of the general base Glu 43 in the enzyme is thus similar to that which one would expect from a corresponding general base in solution (see, e.g., Figure 3 of ref 5). A further reduction of the free energy cost of the proton-transfer step is therefore necessary in order for the enzyme to be able to work at all, and the Ca^{2+} ion must clearly be important in this sense.[5]

The strategy of the present work is to calculate the change in free energy of the enzyme–substrate–ion–water system (at different configurations along the reaction path) associated with substituting Ca^{2+} for other divalent cations. For this purpose FEP/MD simulations are most useful since they allow one to gradually transform a given ion into another, while recording the free energy change of the system. For a given configuration (see below), the only parameters that need to be varied are the nonbonded parameters of the ion interactions, and the free energy can be directly obtained as a function of these. In order to examine the catalytic effects of "mutating" the Ca^{2+} ion, at its site in the protein, we basically need to monitor the free energy change for three different states along the reaction pathway (see ref 5 for details). These are as follows: (i) the reactant state before the proton-transfer step, denoted Ψ_1 (in accordance with the notation in ref 5); (ii) the intermediate state, resulting from step I in which the hydroxide ion has become ligated to the metal, Ψ_2; (iii) the (rate-limiting) transition state associated with forming the pentacoordinated phosphate group, $\Psi^{\ddagger}_{2\rightarrow3}$. Figure 1 shows the three EVB "resonance structures" used to describe the catalytic reaction of SNase. Here, Ψ_3 denotes the pentacoordinated 5′-phosphate group resulting from the attack by OH^-. The transition state $\Psi^{\ddagger}_{2\rightarrow3}$ is obtained in terms of the FEP mixing parameter as the highest point of the free energy profile. Our earlier calculations gave a free energy change of $\Delta G(\Psi_1 \rightarrow \Psi_2) \approx 1$ kcal/mol for the proton-transfer step (with a separating barrier that does not affect the overall rate), while the free energy associated with forming the rate-limiting transition state was $\Delta G(\Psi_2 \rightarrow \Psi^{\ddagger}_{2\rightarrow3}) \approx 14$ kcal/mol, giving an overall activation barrier of $\Delta G^{\ddagger}_{cat} \approx 15$ kcal/mol. If we denote the free energy of changing Ca^{2+} to Me^{2+} (where

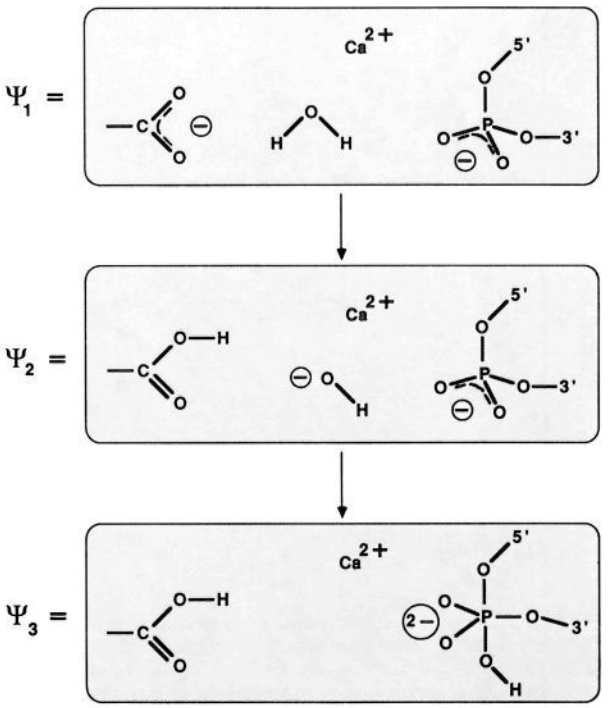

Figure 1. Three EVB resonance structures (Ψ_1, Ψ_2, Ψ_3) used to describe the catalytic reaction of SNase. The first two steps of the mechanism are described by $\Psi_1 \rightarrow \Psi_2 \rightarrow \Psi_3$.

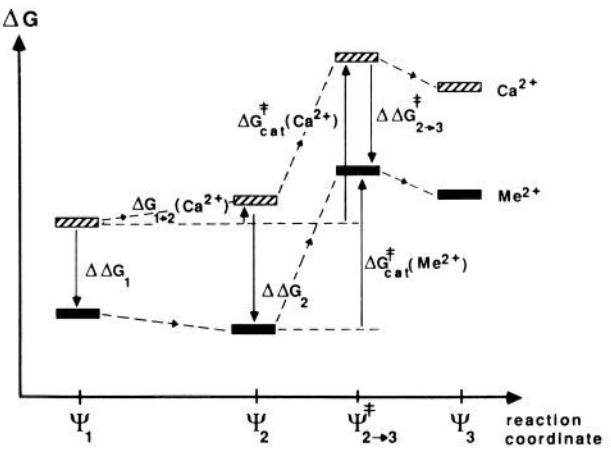

Figure 2. Schematic representation of the change in the overall activation energy, $\Delta G^{\ddagger}_{cat}$, caused by replacing Ca^{2+} by another metal ion. In the depicted case, the solvation energy of Me^{2+} is lower than that of Ca^{2+}.

Me^{2+} can be in either the Sr^{2+} or the Mg^{2+} direction) for these states by $\Delta\Delta G_1(Ca^{2+} \rightarrow Me^{2+})$, $\Delta\Delta G_2(Ca^{2+} \rightarrow Me^{2+})$, and $\Delta\Delta G^{\ddagger}_{2\rightarrow3}(Ca^{2+} \rightarrow Me^{2+})$, the change in the overall activation barrier is given by

$$\Delta\Delta G^{\ddagger}_{cat}(Ca^{2+} \rightarrow Me^{2+}) = \Delta\Delta G^{\ddagger}_{2\rightarrow3}(Ca^{2+} \rightarrow Me^{2+}) - \min[\Delta\Delta G_1(Ca^{2+} \rightarrow Me^{2+}), \Delta\Delta G_2(Ca^{2+} \rightarrow Me^{2+}) + \Delta G_{1\rightarrow2}(Ca^{2+})] \qquad (2)$$

where $\Delta G_{1\rightarrow2}(Ca^{2+}) \approx 1$ kcal/mol. This relation is depicted diagramatically in Figure 2 for the case of Me^{2+} being an ion with lower hydration energy than Ca^{2+} (i.e., all the $\Delta\Delta G$'s are negative).

The potential parameters used in the present calculations are identical with those of ref 5. The ion interacts via electrostatic and Lennard-Jones terms, $V_{Ij} = 332Q_Iq_j/r_{Ij} + A_IA_j/r_{Ij}^{12} - B_IB_j/r_{Ij}^6$, where the subscript I denotes the ion and j is another atom with which it interacts. The nonbonded Ca^{2+} parameters were determined previously[5] by performing FEP/MD calculations on the solvated ion, requiring that both the experimentally observed radical distribution function[11] and hydration free

(7) (a) Tucker, P. W.; Hazen, E. E., Jr.; Cotton, F. A. *Mol. Cell. Biochem.* **1979**, *23*, 67–86. (b) Cotton, F. A.; Hazen, E. E., Jr.; Legg, M. J. *Proc. Natl. Acad. Sci. U.S.A.* **1979**, *76*, 2551–2555. (c) Loll, P. J.; Lattman, E. E. *Proteins* **1989**, *5*, 183–201.

(8) Wilde, J. A.; Bolton, P. H.; Dell'Acqua, M.; Hibler, D. W.; Pourmotabbed, T.; Gerlt, J. A. *Biochemistry* **1988**, *27*, 4127–4132.

(9) Tucker, P. W.; Hazen, E. E., Jr.; Cotton, F. A. *Mol. Cell. Biochem.* **1978**, *22*, 67–77.

(10) Guthrie, J. P. *J. Am. Chem. Soc.* **1977**, *99*, 3991–4001.

(11) Licheri, G.; Piccaluga, G.; Pinna, G. *J. Chem. Phys.* **1976**, *64*, 2437–2441.

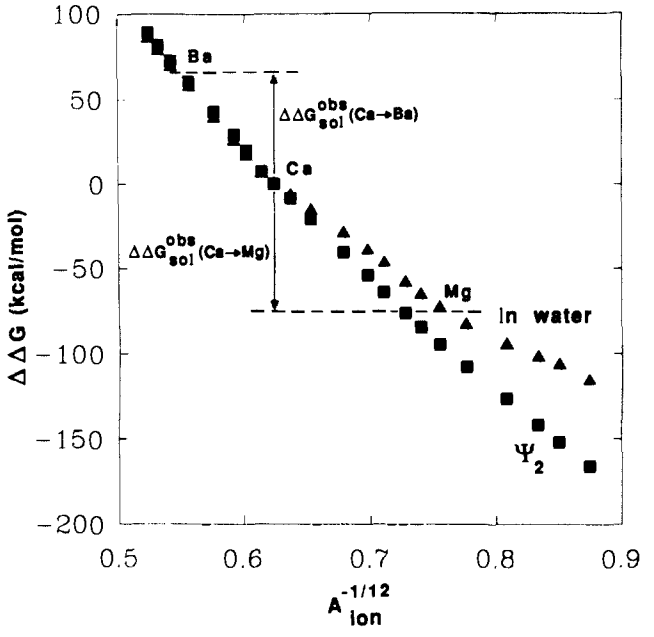

Figure 3. Calculated free energy changes associated with transforming Ca^{2+} to ions with different radii, in water (triangles) and in the state Ψ_2 in the enzyme's active site (squares). The nonbonded Lennard-Jones parameter A_{ion} is approximately related to the effective ion radius by $A_{ion}^{1/12} \approx k(r_{ion} + r_{water})$. The observed hydration energy differences between Ba^{2+}, Ca^{2+}, and Mg^{2+} are also indicated.

energy be reproduced (for a compilation of observed ion solvation free energies, see ref 12). In order to calibrate the calculated hydration energies for different ions versus the nonbonded parameters, we first carry out FEP/MD simulations of a solvated ion in water. In these calculations the Lennard-Jones parameters of the ion were gradually changed from $(A_I, B_I) = (2340.0, 25.0)$ to $(A_I, B_I) = (5.0, 1.0)$. This range of parameters was found to cover ions from beyond Ra^{2+} to somewhere in between Mg^{2+} and Be^{2+} (see below). These calibration calculations in water covered a total simulation time of 40 ps for both the forward and backward transformation direction. The solvent was represented by the SCAAS (surface constraint all atom solvent) model[13] in all calculations reported here.

The same calculation is then performed with the ion in the active site of SNase for each of the three states Ψ_1, Ψ_2, and $\Psi^{\ddagger}_{2\to3}$ (for further details and parameters of the protein calculations, see ref 5). Hence, with the previously calculated energy profile for Ca^{2+} we can directly obtain the difference in $\Delta\Delta G^{\ddagger}_{cat}$ from the free energy changes of the three states as a function of the metal ion parameters.

Results

As mentioned above, we must start by calibrating the ion interaction parameters versus the free energy hydration. Without the calibration of these parameters in water it would not be possible to make meaningful comparisons to experimental data. If one were to use, for example, ab initio potentials for the ion interactions without verifying that these reproduce the observed hydration energies, attempts to make quantitative comparisons to kinetic data would involve significant uncertainties.

The calibration procedure is quite straightforward for the alkaline-earth metals, and these ions can be reasonably well modeled by simple charged Lennard-Jones spheres. That is, the nonbonded parameters can be adjusted so that the solvation energy and the first peak of the radial distribution function (RDF) in water coincide with experimental values. For transition metals, however, the situation becomes more complicated, and we will return to this issue below. The calculated solvation free energies in water (relative to that of Ca^{2+}) are shown in Figure 3. Te quantity $\Delta\Delta G_{sol}(Ca^{2+} \to Me^{2+})$ is plotted versus the ion repulsive nonbonded parameter, which effectively determines the radius of the ion (although the RDF for each set of nonbonded parameters can be caculated, we have chosen to represent the inverse of the ion size by $A_{ion}^{-1/12}$ since these are explicit parameters in the FEP/MD simulations. The value of A_{ion} is approximately related to the ion size by $A_{ion}^{1/12} \approx k[r_{ion} + r_{water}]$.) The calculated $\Delta\Delta G_{sol}$ curve in water together with the corresponding observed values, thus, define the scale of ion parameters in terms of solvation energies. For comparison, the same calculation in the configuration corresponding to the state Ψ_2 in the enzyme is also presented in Figure 3. Since the active site of SNase provides several metal ligands with net charges, in particular in the state Ψ_2 that contains a free (unbound) hydroxide ion, one would expect the protein microenvironment to be a "stronger" solvent for the metal than water. This is also reflected by the fact that several divalent metal ions bind strongly to the active site.[3b,4] Another way of putting it is that we would expect the curve $\Delta\Delta G_2$ to have a curvature different from that of $\Delta\Delta G_{sol}$. This is also the result that emerges from the FEP/MD calculations, and as expected, the change in solvation free energy between any two given ion radii is larger for this state in the protein than it is in water (Figure 3).

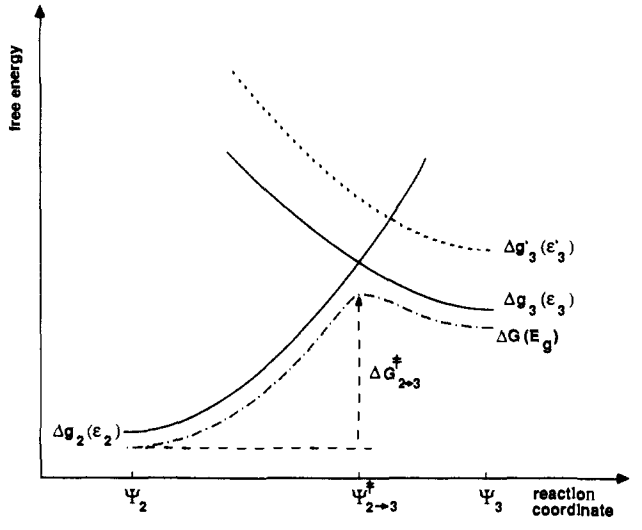

Figure 4. Demonstration of the correlation between the ground-state activation free energy ($\Delta G^{\ddagger}$) and the height of the intersection between free energy functionals of the diabatic surfaces in a two-state reaction model. If the curve Δg_3 that describes the free energy of the state Ψ_3 is shifted relative to Δg_2 as shown in the figure, the activation energy (i.e., the relative energy of the transition state $\Psi^{\ddagger}_{2\to3}$) will increase approximately by $\Delta\Delta G^{\ddagger}_{2\to3}[E_g] = \Delta g_3'(X) - \Delta g_3(X) + \Delta\Delta g_3(X^{\ddagger} \to X^{\ddagger'})$, since E_g is given by $E_g = {}^1/_2(\epsilon_2 + \epsilon_3) - {}^1/_2((\epsilon_2 - \epsilon_3)^2 + 4H^2_{12})^{1/2}$ (X denotes the reaction coordinate).

(a) Free Energy Relationships for the Catalytic Reaction of SNase. With some qualitatative confidence about our potential parameters, we may start exploring the catalytic effect of substituting the active site Ca^{2+} ion in SNase. As a first step, it is useful to examine the role of the metal in a simple two-state reaction model in which the state Ψ_2 is of lower energy than Ψ_1 for all divalent ions. It is then only the free energies of Ψ_2 and $\Psi^{\ddagger}_{2\to3}$ that determine the rate of the catalytic reaction, if we assume that ion binding is always "downhill". This simplified reaction model (which will later be extended to the actual reaction) allows us to present the main conceptually limiting cases in terms of simple linear free energy relationships. In other words, with the two states Ψ_2 and Ψ_3 we can examine the correlation between the activation free energy ($\Psi^{\ddagger}_{2\to3}$ in this model) of the reaction and the energy of Ψ_2 and Ψ_3 in terms of the diagram given in Figure 4. As seen from the figure, the transition state of the ground-state potential surface (obtained from the mixing of Ψ_2 and Ψ_3) will be strongly correlated with the height of the intersection between the free energy functionals corresponding to the diabatic surfaces (Δg_2 and Δg_3) of Ψ_2 and Ψ_3. If the minimum of Δg_2 is pushed down relative to that of Δg_3, then $\Delta G^{\ddagger}_{2\to3}$ (which corresponds to the adiabatic ground state E_g) will increase, while if the minimum

(12) Burgess, M. A. *Metal Ions in Solution*; Ellis Horwood Ltd.: Chichester, England, 1978.

(13) (a) Warshel, A.; King, G. *Chem. Phys. Lett.* **1985**, *121*, 124–129. (b) King, G.; Warshel, A. *J. Chem. Phys.* **1988**, *91*, 3647–3661.

of Δg_3 is pushed down, it will decrease. The difference in solvation energy between different ions will, of course, result in a shift of the absolute free energies of Ψ_2 and Ψ_3 (given by the curves Δg_2 and Δg_3) if a given ion is replaced by another. Moreover, it is likely that the energies of the two states are not equally affected by the ion substitution, and this would therefore also give a relative shift between the two free energy curves, as indicated in Figure 4 (for a general examination of such free energy relationships in solutions and in proteins, see ref 26).

We would thus expect a few basic tpes of "selectivity" patterns for the rate constant (Figure 5a–d) as a consequence of different sensitivities between the two states to the ion properties. The changes in "solvation" free energy of the states Ψ_2 and Ψ_3 as a function of metal ion are plotted in Figure 5 relative to an arbitrary ion. In order to make the discussion less abstract we will call this reference ion Ca^{2+}, but this choice is completely arbitrary and does not involve any assumptions concerning the nature of the two states; it simply serves as to define a scale for the ion size. The four cases depicted correspond to different relations between the curvatures of $\Delta\Delta G_2(1/r_{ion})$ and $\Delta\Delta G_3(1/r_{ion})$. In Figure 5a, Ψ_3 is less sensitive to the ion size than Ψ_2 over the entire range of r_{ion}. Hence, the larger the ion the larger the rate constant will be, $k(Ba^{2+}) > k(Ca^{2+}) > k(Mg^{2+})$. If, on the other hand, Ψ_2 is less sensitive to the ion radius we will obtain the opposite ordering between the rates, $k(Ba^{2+}) < k(Ca^{2+}) < k(Mg^{2+})$ (Figure 5b). As a third case one can imagine the possibility that Ψ_2 is more sensitive to larger ions while Ψ_3 is more sensitive to smaller ions. This case is depicted in Figure 5c and would lead to a maximum of the activation barrier for the intermediate ion, $k(Ba^{2+}) > k(Ca^{2+}) < k(Mg^{2+})$. The only case that could give a minimum barrier for the intermediate ion is shown in Figure 5d, in which the sensitivities of the states in Figure 5c have been reversed. Here, the ordering between the rate constants would be $k(Ba^{2+}) < k(Ca^{2+}) > k(Mg^{2+})$, and the enzyme could thus be said to be opimized for the intermediate ion. A discussion similar to that presented above has been given by Eisenman and Horn[14] in the rather different context of selectivity ion channels. It can be noted that the so-called Eisenman selectivity sequences arise from the relations between the curvatures of ion hydration and the binding free energy as a function of the ion size. Although not included in our examples above, one can also image "anomalous" selectivity patterns that would result if one of the $\Delta\Delta G$ curves has an inflection point (i.e., a change of sign of the curvature).

In Figure 6 the actual results of FEP/MD calculations for the states Ψ_2 and $\Psi^*_{2\rightarrow3}$ along the reaction coordinate are shown. Instead of plotting the free energy of Ψ_3, which does not directly give us the change in activation barrier, the free energy of the transition state $\Psi^*_{2\rightarrow3}$ is depicted in Figure 6. This does, however, not change the general picture outlined above, since $\Psi^*_{2\rightarrow3}$ can be viewed as a mixture of Ψ_2 and Ψ_3 [the system is constrained to be in the transition-state region by the mapping poential $\epsilon^*_{2\rightarrow3} = \epsilon_2\lambda^*_2 + \epsilon_3\lambda^*_3 - 2|H_{23}|(\lambda^*_2\lambda^*_3)^{1/2}$, where $\bar{\lambda} = (\lambda_1, \lambda_2, \lambda_3)$ is the mapping parameter (for further details, see ref 5)]. It can be seen that the relationship between $\Delta\Delta G_2$ and $\Delta\Delta G^*_{2\rightarrow3}$ most resembles the last of the four cases considered above. The influence of the state Ψ_1 (not shown) on $\Delta\Delta G^*_{cat}$ is rather small since $\Delta\Delta G_1 \approx \Delta\Delta G_2$ for ions larger than Ca^{2+} and $|\Delta\Delta G_1| < |\Delta\Delta G_2|$ for the smaller ions.

The origin of the dependencies of $\Delta\Delta G_2$ and $\Delta\Delta G^*_{2\rightarrow3}$ on r_{ion} can be rationalized in the following way. When the smaller metals are bound to the enzyme, the free energy of Ψ_2 will be lowered considerably more than that of the transition state (as well as Ψ_3) since in the former the OH^- ion is free to interact with or ligate the metal, while it is becoming partially bound to the 5′-P atom at the transition state with accompanying charge delocalization.[28] On the other hand, when the metal ion becomes too large, it has less ability to perform its other major catalytic role (besides stabilizing the hydroxide ion in the first reaction step), namely, solvating the developing double-negative charge on the phosphate group. That is, for the larger ions the state $\Psi^*_{2\rightarrow3}$ would be more sensitive to the ion size than Ψ_2 because of the less efficient solvation of the phosphate group.

After calculating the ion size dependence of the $\Delta\Delta G$'s, we can evaluate the effect of metal substitution on the catalytic rate. By inserting the calculated quantities $\Delta\Delta G_1(Ca^{2+} \rightarrow Me^{2+})$, $\Delta\Delta G_2(Ca^{2+} \rightarrow Me^{2+})$, and $\Delta\Delta G^*_{2\rightarrow3}(Ca^{2+} \rightarrow Me^{2+})$, in eq 2, we obtain the overall change in activation energy (relative to Ca^{2+}) as a function of the ion size. The resulting free energy diagram is presented in Figure 7, where the locations of Sr^{2+}, Ba^{2+}, Ca^{2+}, and Mg^{2+} have been indicated on the curve. The two main conclusions to be drawn from the dependence of $\Delta\Delta G^*_{cat}$ on the ion radius are as follows: First, there is a clear minimum in the neighborhood of Ca^{2+}, which suggests that the enzyme has been optimized to work exactly with calcium bound. Second, it can be noted that the calculated effect on the catalytic rate is more pronounced when a smaller ion, such as Mg^{2+}, replaces Ca^{2+} than is the case for the larger Sr^{2+} and Ba^{2+} ions (see also ref 28). This appears mainly to be due to the fact that $\Delta\Delta G_2$ departs from the corresponding free energy change of the two other states for smaller ions, while the free energy of all three states show a more commensurable behavior for larger ions.

The trend in $\Delta\Delta G^*_{cat}$ for the alkaline-earth metals appears to agree with the experimental observations by Cuatrecasas et al.[4] These authors found no enzyme activity when Ca^{2+} was substituted for Mg^{2+}, while some of the activity was retained with DNA as substrate when Sr^{2+} was bound to be the enzyme (14, 60, and 40% of the Ca^{2+} activity at 0.1, 1, and 10 mM ion concentrations, respectively).

However, the reported results[4] appear somewhat inconsistent with respect to the transition-metal ions. While no enzymatic activity was observed for Cd^{2+}, Hg^{2+}, Mn^{2+}, Co^{2+}, Zn^{2+}, and Ni^{2+}, surprisingly, some activity was retained with Fe^{2+} (6%) and Cu^{2+} (10%), but only at one particular ion concentration (0.1 mM). Since it seems likely that the catalytic rate is directly related to the ion hydration free energies or acidities, the reported activities for Fe^{2+} and Cu^{2+} appear somewhat obscure (later experiments[16b] on deoxyribonuclease I have demonstrated that traces of Ca^{2+} in several bivalent metal salts can account for comparable activities). Apparently, the most reliable measurements of the enzyme activity with other ions bound are those reported in ref 3b. These authors found that Mn^{2+} and Co^{2+} were at least a factor of 36 000 less efficient than Ca^{2+} in activating the enzyme and also acted as competitive inhibitors with the latter.

(b) Treatment of Transition Metals. In addition to the alkaline-earth metal ions, which lack d-orbital valence electrons, it is important to try to extend the applicability of our model to include also transition metals. Unfortunately, the hydration energies of the transition-metal ions cannot be well modeled by a simple Lennard-Jones sphere with a charge in the center; in order to reproduce the observed hydration energy the ion radius must be made too small to be compatible with the observed one. Manifestations of ligand field effects lead to a more complicated pattern of solvation energies for the transition-metal ions (the differences in hydration energy among these ions can be directly related to the crystal field stabilization energies). All of the divalent transition metals have lower (more negative) hydration energies than an alkaline-earth ion of the same radius would have (we say would since the latter type of ion only comes in a limited number of versions and one must interpolate between these). It is thus clear that in order to model these ions in microscopic simulations one must resort to more sophisticated models than simple charged spheres. We have attempted in a preliminary way to model the Mn^{2+} ion in order to obtain a comparison with the experiments of Sepersu et al.[3b]

Our model for Mn^{2+} (which has some theoretical justification, as will be argued below) corresponds to adding six fractional positive charges, $+\delta$, in octahedral geometry at a distance r_δ from

(14) Eisenman, G.; Horn, R. *J. Membr. Biol.* **1983**, *76*, 197–225.
(15) Sepersu, E. H.; McCracken, J.; Peisach, J.; Mildvan, A. S. *Biochemistry* **1988**, *27*, 8034–8044.
(16) (a) Suck, D.; Oefner, C. *Nature (London)* **1986**, *321*, 620–625. (b) Price, P. A. *J. Biol. Chem.* **1975**, *250*, 1981–1986.

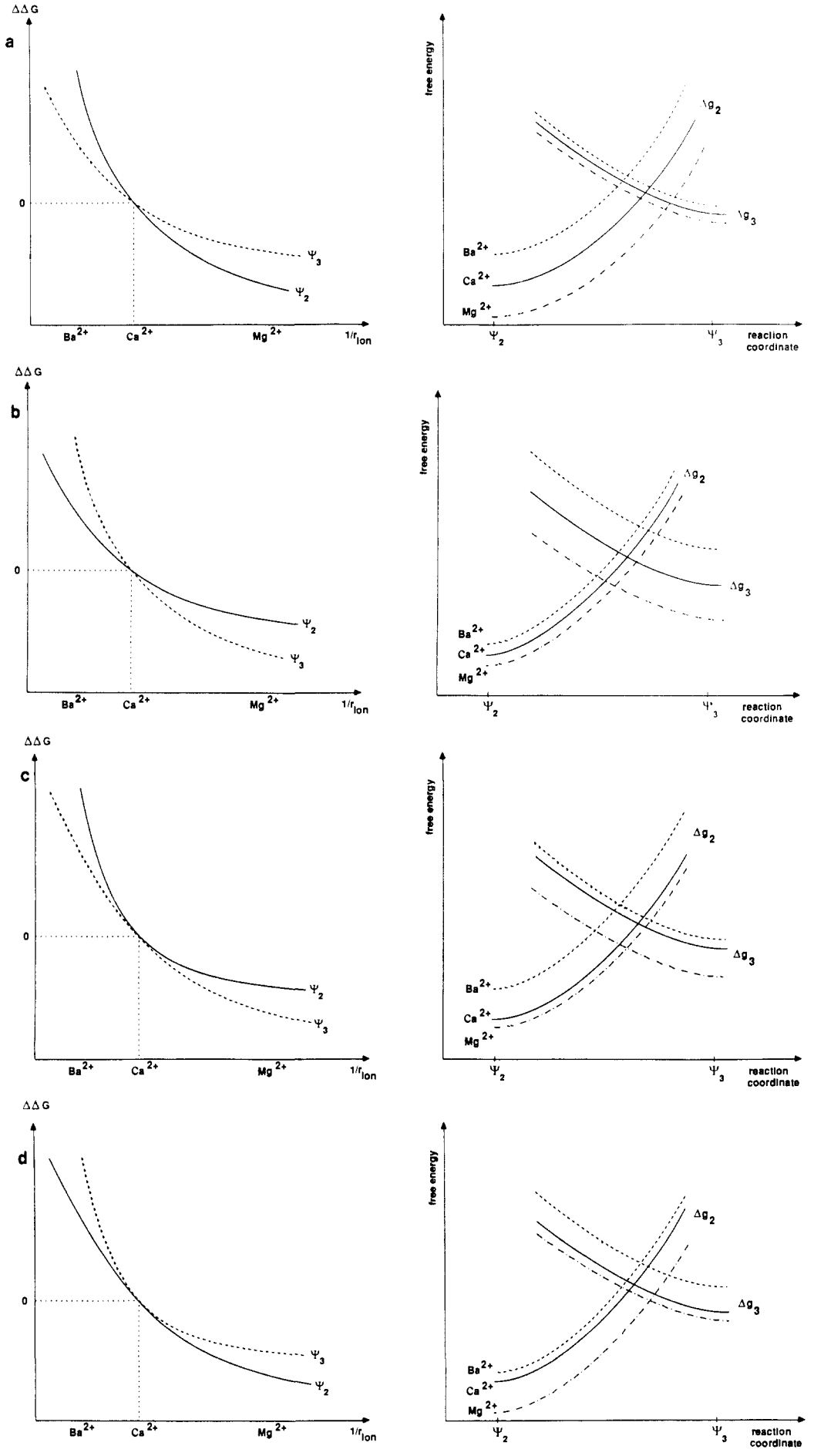

Figure 5. Schematic description of how the dependence of the free energy of the two states Ψ_2 and Ψ_3 on the size of the bound metal ion can give rise to different rate "selectivities". The leftmost diagram in each of the four cases (a–d) shows how the free energy of each state changes (relative to an arbitrary ion, which we call Ca^{2+}) as a function of ion radius. The right-most diagram in each case demonstrates how the particular free energy dependences of Ψ_2 and Ψ_3 give rise to different relations between the reaction profiles for different ions (only the diabatic energy surfaces are drawn).

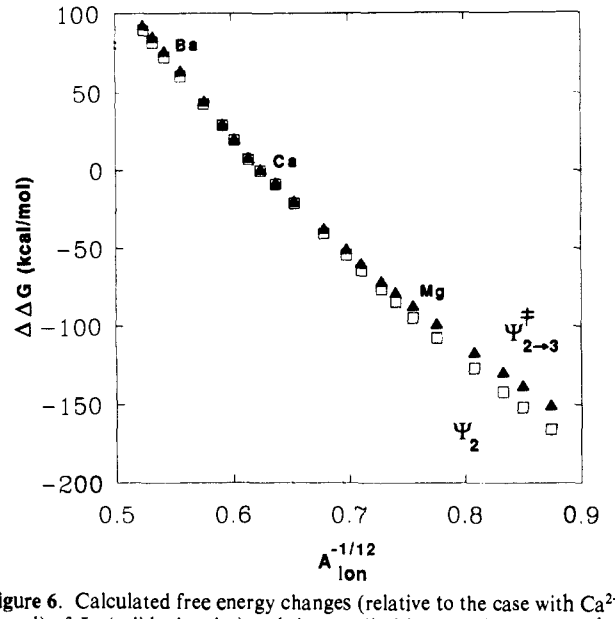

Figure 6. Calculated free energy changes (relative to the case with Ca^{2+} bound) of Ψ_2 (solid triangles) and the rate-limiting transition state $\Psi^{\ddagger}_{2\rightarrow3}$ (open squares) as a function of the repulsive nonbonded parameter.

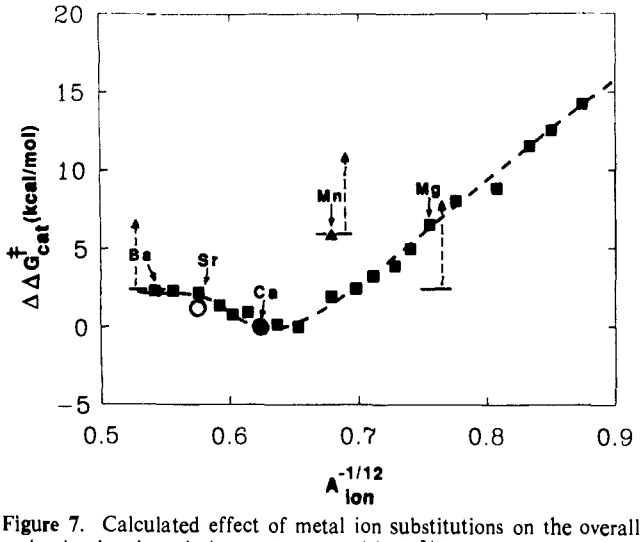

Figure 7. Calculated effect of metal ion substitutions on the overall activation barrier relative to the case with Ca^{2+} bound. Each point is calculated according to eq 2 from the quantities $\Delta\Delta G_1$, $\Delta\Delta G_2$, $\Delta\Delta G^{\ddagger}_{2\rightarrow3}$, and $\Delta G_{1\rightarrow2}(Ca^{2+})$. The value of $\Delta\Delta G^{\ddagger}_{cat}$ for Mn^{2+} is plotted above a "spherical" ion with the same radius (as given by the RDF), so that the value of A_{ion} corresponds to that of the latter ion and not to the actual value used for Mn^{2+}. The observed values for Sr^{2+} and Ca^{2+} are denoted by circles and experimentally estimated limits for Ba^{2+}, Mg^{2+}, and Mn^{2+} by ↑.

the center of the ion and a corresponding charge of -6δ in the center, thus retaining a net charge of +2. The ion then interacts with One Lennard-Jones center (at the center of the ion) and seven electrostatic centers; the geometry of the six peripheral fractional charges is rigid, but overall rotation of the six-center frame about the nucleus is allowed, and no internal forces are associated with such rotations. The model parameters used here for Mn^{2+} are as follows: $(A_1, B_1) = (145.0, 25.0)$, $\delta = 0.35$, $r_\delta = 0.9$ Å. These parameters reproduce the observed hydration energy and simultaneously give a radial distribution function in accordance with the observed ionic radius. Apparently this empirical model retains some of the basic characteristics of the Mn^{2+} ion in solution (and also in the SNase active site environment[15]). That is, the model simulates the preference of transition metals (relative to simple spherical ions) for an octahedral geometry by its specific charge distribution. Furthermore, this type of charge distribution leads to an increase of the (absolute value) calculated hydration energy compared to an alkaline-earth ion with the same effective radius. On the basis of ligand field theory, one would expect the electron density to be partly shifted to the d orbitals along the bisectors between the ligands, so that the screening of the nuclear charge becomes smaller in the ligand directions than in the case of a "spherical" ion. This situation is described by our model in a rather crude fashion (one could perhaps achieve an improvement by representing all 18 bisector and ligand directions with explicit charges, which would be determined according to ligand field theory prescriptions, but for the present purpose the seven-center model seems satisfactory).

The calibration of the Mn^{2+} parameters in solution was done by gradually perturbing a Ca^{2+} ion into Mn^{2+} and calculating the change in hydration free energy associated with the transformation. The experimental value for $\Delta G_{sol}(Ca^{2+}) - \Delta G_{sol}(Mn^{2+})$ is −57 kcal/mol (see, e.g., ref 12), while the corresponding calculated number in water for our model is −59 kcal/mol. These calibrated parameters were then used to calculate the effect of a corresponding ion transformation, for each of the three relevant states along the reaction coordinate, in the protein environment. The calculated effect of a Mn^{2+} ion on the overall activation barrier of the enzyme is shown in Figure 7. The value of $\Delta\Delta G^{\ddagger}_{cat}$ for Mn^{2+} is plotted above the corresponding spherical ion, which has the same radius as Mn^{2+} (i.e., the value of the repulsive Lennard-Jones parameters refers to the spherical ion and not to Mn^{2+}).

As discussed above, the main reason for the relatively sharp increase in activation energy as Ca^{2+} is transformed to smaller ions (cf. Figure 7) is that the free energy of Ψ_2 is lowered more than that of the transition state.[28] The effect is much more pronounced for Mn^{2+} (as represented by our model) than for a corresponding hypothetical alkaline-earth-like ion of the same radius. Furthermore, if one considers a spherical ion with the same calculated hydration energy as that of Mn^{2+}, the latter gives a value of $\Delta\Delta G^{\ddagger}_{cat}$ that is about 2 kcal/mol higher. The calculated change in the overall activation barrier, $\Delta\Delta G^{\ddagger}_{cat}(Ca^{2+} \rightarrow Mn^{2+})$, is about 6 (±1) kcal/mol. This value agrees fairly well with the experimental observation[3a,b] that Mn^{2+} is at least a factor of 36000 less efficient as an activator than Ca^{2+}.

We have not addressed the issue of ion binding to the enzyme in the present study. This would require a higher accuracy for the calculated ion solvation energies in water than that presently attained. The convergence errors of the FEP/MD calibrations in water when, e.g., a Ca^{2+} ion is transformed to Mn^{2+}, are about 3–4 kcal/mol, which is a rather large number compared to the free energies of ion binding, and the thermodynamic cycle used for obtaining binding energies requires very accurate calculations in water. However, the convergence errors in the protein calculations are (at least in the present case) almost 1 order of magnitude smaller than in water. The reason why the differential binding in the enzyme seems to be more easily modeled is probably due to the fact that the active site is strongly polarized toward the charge (there are several negatively charged groups in the innermost coordination spheres of the metal). Apparently, the difficulties in studying divalent ions are largely due to their high solvation energies. To reach a higher accuracy in the water calibration procedure one would presumably have to use a larger system as well as longer simulations. However, the binding step clearly does not affect the overall rate for Ca^{2+} and the smaller ions, since the binding is "downhill" in these cases.[3a,b] For the larger ions Sr^{2+} and Ba^{2+} no binding data are available, but the present calculations indicate that the binding of these ions to the enzyme is slightly weaker than for Ca^{2+} and that the ordering between the binding constants follows the ion size, i.e., $K^{Ca}_{bind} > K^{Sr}_{bind} > K^{Ba}_{bind}$.

Concluding Discussion

The present work indicates that is is possible to examine the catalytic role of metal ions in enzymes by computer simulation methods in a semiquantitative way, with quite simple potential energy functions for the ionic interactions. It is encouraging to note that, to the extent that experimental data are available, the calculated changes in the activation energy agree reasonably well with kinetic measurements. In particular, it appears that even

transition metals, which involve more quantum mechanical subtilities than is the case of ions with no valence d electrons, can be fairly well modeled by simple potentials such as that used here for Mn^{2+}.

It is also interesting to note that our results indicate that SNase is indeed optimized to work with Ca^{2+} as its catalytic ion. This optimum arises both from the requirement that the energetic cost of the proton-transfer step should be as low as possible without "trapping" the hydroxide ion in a too deep (electrostatic) well as well as from the neccessity of attaining a strong solvation of the accumulating negative charge on the 5′-phosphate group at the transition state. Furthermore, as Figure 7 suggests, the enzyme appears to be more sensitive to ions with larger (than with smaller) hydration energies compared to Ca^{2+}, since these interact more strongly with the intermediately created OH^- ion, making the nucleophilic attack more difficult.

The finding that SNase appears to have its turnover optimum for the ion, which it in fact uses in nature, may, of course, be considered not terribly surprising. However, the free energy relationships leading to a rate optimization are quite interesting and point toward more general features that may pertain also to other metalloenzymes, with both similar as well as quite different catalytic reactions. Perhaps the most immediate example is that of deoxyribonuclease I (DNase I). This enzyme catalyzes essentially the same reaction as SNase with presumably the same mechanistic pathway.[16a] The main difference appears to be that while SNase uses a glutamate as the general base, DNase I has instead chosen a histidine residue (His 131) for this step. The dependence of the catalytic rate of DNase I on replacement of the Ca^{2+} ion by various other divalent metal ions has also been studied.[16b] The influence of these replacements on the activity of the enzyme agrees qualitatively well with the calculated $\Delta\Delta G^{\ddagger}_{cat}$ curve for SNase (Figure 7). Only Sr^{2+} and Ba^{2+} can replace the catalytic calcium ion in DNase I, but they are less effective (Ba^{2+} more so that Sr^{2+}).[16b]

Another example with similar mechanistic features, but for a different reaction, is the catalysis of ester bond hydrolysis in phospoglycerides by phospholipase A_2.[17] As for SNase and DNase I, phospholipase also has an absolute requirement for Ca^{2+} as a cofactor, and the Ca^{2+} appears to play a very similar role to that in SNase. It binds the negatively charged substrate phosphate group and probably also facilitates the abstraction of a proton to yield the OH^- nucleophile. Furthermore, it must be important for stabilizing the charges of the tetrahedrally coordinated C2 carbon transition state, in analogy with its multiple tasks in SNase. The proposed mechanism[17a] for phospholipase A_2 also involves general-base-assisted catalysis in the first step of the reaction through an Asp–His pair similar to that found in the serine proteases (as well as DNase I). Several divalent metal ions have been shown to be inhibitory, and no cation has been found that can replace Ca^{2+} in the enzymatic reaction.[18] Since both Sr^{2+} and Ba^{2+} form ternary enzyme–metal–substrate complexes with phospholipase A_2, but neither ion promotes catalysis, it was suggested[17a] that only Ca^{2+} can effectively enhance polarization of the ester carbonyl oxygen in the second reaction step. Thus, the reduced ability (compared to Ca^{2+}) for these larger ions to "solvate" the negatively charged transition state appears to provide a rationalization of the data for phospholipase A_2 also, in manner similar to SNase (a less efficient stabilization of the OH^- nucleophile could also contribute to the absence of activity for these ion). However, the argument above cannot account for why the more electrophilic ions do not promote catalysis. For these ions, the inability to activate the enzyme may again reflect a strong interaction between the metal and the nucleophile, which hampers its possibility to attack the substrate.

Similar reaction mechanisms, involving general-base and metal ion catalysis, in conjunction with OH^- nucleophile attack, have been proposed for thermolysin[19] and carboxypeptidase A.[19,20] Both enzymes use Zn^{2+} as their catalytic metal, and they also have additional positively charged active site residues (His 231 in thermolysin and Arg 127 in carboxypeptidase) with, presumably, similar transition-state stabilization effects as the arginines in SNase, DNase I, and alkaline phosphatase. It is noteworthy that thermolysin and carboxypeptidase, as opposed to the previous cases, combine the choice of the stronger Zn^{2+} ion with general-base catalysis (by a glutamate), if the proposed mechanisms for these enzymes are correct. Metal substitution experiments[21] on carboxypeptidase A have shown that the activity is optimal with Zn^{2+} or Co^{2+} bound. In this case the alkaline-earth metals produce no activity.[21] Interestingly, it appears that carboxypeptidase A is more sensitive to replacement by transition metals with larger hydration energy than cobalt and zinc than by those with smaller hydration energies. This might be indicative of a free energy relationship similar to Figure 7, underlying the observed optimum for Co^{2+} and Zn^{2+}. As a final example, one can mention the more unrelated reactions catalyzed by carbonic anhydrase and alcohol dehydrogenase (ADH), which both are zinc enzymes. In the former case, the main role of the catalytic Zn^{2+} ion appears to be lower the pK_a of the reacting water molecule, which is ligated to the ion, as well as binding the substrate,[22,23] much in the same manner as discussed above. The catalytic efficiency of different fourth-row metal ions in carbonic anhydrase also approximately follows the hydration energy scale from Ca^{2+} (which gives no activity) to an optimal turnover for Zn^{2+} and then vanishes rapidly (Ni^{2+} gives about 5% of the Zn^{2+} activity, and the Cu^{2+} enzyme is inactive).[24] It should be noted, however, that the acidity of the transition metal does not strictly follow the hydration energy (or ion radius) scale. Furthermore, the highly acidic Hg^{2+} and Cu^{2+} ions were proposed[24] to bind to a site distinct from the catalytic Zn^{2+} site since they inhibit the exchange of water from the enzyme without affecting the equilibrium rate of hydration of CO_2 (the crystallographic structure of the Hg^{2+} inhibited isozyme II, reported in ref 23, confirms this proposal).

The mechanistic features of the ADH-catalyzed reaction differ somewhat from the previous cases, since the step following the alcohol deprotonation involves a hydride transfer[25] instead of an $R-O^-$ nucleophilic attack. However, the deprotonation of the alcohol group corresponds to basically the same energetics *in solution* as the first step of the previous cases. That is, the free energy cost of transferring the proton to a water molecule *in solution* is about 22 kcal/mol. Therefore, the enzyme must be able to reduce the energetic cost of about 22 kcal/mol to a much more tractable number in order to accomplish any catalysis at all. In this respect, it again appears that the Zn^{2+} ion bears the heaviest burden in catalyzing the first step of the reaction.[25]

In all of the cases discussed above, the metal ion plays a central role in facilitating an otherwise unfavorable proton-transfer step as well as for subsequent transition-state stabilization and substrate binding. As for the first point above, it should be kept in mind that, even with a general base (as opposed to a water molecule) to accept a proton from a water molecule, the cost of forming an OH^- nucleophile is about 11–16 kcal/mol *in solution* depending

(17) (a) Verheij, H. M.; Volwerk, J. J.; Jansen, E. H. J. M.; Puyk, W. C.; Dijkstra, B. W.; Drenth, J.; de Haaas, G. H. *Biochemistry* **1980**, *19*, 743–750. (b) Dijkstra, B. W.; Drenth, J.; Kalk, K. H. *Nature (London)* **1981**, 604–606.
(18) Wells, M. A. *Biochemistry* **1972**, *11*, 1030–1041.
(19) Matthews, B. W. *Acc. Chem. Res.* **1988**, *21*, 333–340.
(20) Christianson, D. W.; David, P. R.; Lipscomb, W. N. *Proc. Natl. Acad. Sci. U.S.A.* **1987**, *84*, 1512–1515.
(21) Vallee, B. L.; Galdes, A.; Auld, D. S.; Riordan, J. F. In *Zinc Enzymes*; Spiro, T. G., Ed.; Wiley: New York, 1983; pp 25–75.
(22) Silverman, D. N.; Lindskog, S. *Acc. Chem. Res.* **1988**, *21*, 30–36.
(23) Eriksson, A. E.; Kylsten, P. M.; Jones, T. A.; Liljas, A. *Proteins* **1988**, *4*, 283–293.
(24) Lindskog, S.; Nyman, P. O. *Biochem. Biophys. Acta* **1964**, *64*, 462–474.
(25) (a) Brändén, C.-I.; Eklund, H. In *Dehydrogenases Requiring Nicotinamide Coenzymes*; Jeffery, J., Ed.; Birkhauser: Basel, 1980; pp 41–84. (b) Eklund, H.; Brändén, C.-I. In *Zinc Enzymes*; Spiro, T. G., Ed.; Wiley: New York, 1983; pp 123–152. (c) Tapia, O.; Eklund, H.; Brändén, C.-I. In *Steric Aspects of Biomolecular Interactions*; Náray-Szabó, G., Simon, K., Eds.; CRC Press: Boca Raton, FL, 1987; pp 159–180.
(26) (a) Hwang, J.-K.; King, G.; Creighton, S.; Warshel, A. *J. Am. Chem. Soc.* **1988**, *110*, 5297–5311. (b) Warshel, A.; Russell, S. T.; Sussman, F. *Isr. J. Chem.* **1986**, *27*, 217–224.

on the type of general base (it is about 21 kcal/mol without general-base catalysis). Therefore, the advantage of using a divalent metal ion in order to accelerate the first reaction step is obvious.

On the basis of these examples, it is reasonable to suggest that the underlying principles for optimization of the overall reaction rate with respect to the choice of metal ion are similar (this may not necessarily apply to ADH since the second reaction step is somewhat different from the other reactions). That is, there are basically three states (in addition to the relevant solvation free energies) along the reaction pathway that determine the most suitable choice of metal ion. These are as follows: firstly, the reactant state with bound metal (and possibly substrate) preceding the proton-transfer step; secondly, the intermediately created free OH^- nucleophile; and thirdly, the subsequent transition state associated with the nucleophilic attack. It must clearly be advantageous to reduce the cost of abstracting the proton from the nucleophile as much as possible, but, as elucidated in the case of SNase, a too electrophilic metal is likely to be less efficient by "trapping" the OH^- ion as a ligand. The electrostatic stabilization of the negatively charged transition state is not, at least in the case of SNase, as much affected by chosing a small electrophilic ion with large hydration energy as is the interaction with the free hydroxide ion. This can probably be interpreted as a consequence of the higher degree of charge delocalization at the transition state, where the negative charge carried by the nucleophile is becoming distributed over several atoms.

The optimum activation barrier elicited by our calculations on SNase suggests that one might expect a correlation between the electrophilicity of the metal and the strength of the (general) base for enzymes catalyzing reactions involving a proton-transfer step. Let us, for a moment, consider the energetics of a proton-transfer reaction of the type involved in the first step of the examples above, in solution. Under the influence of a possible general base as the proton acceptor and a possible metal ion assisting as a catalyst we can write

$$\text{R–OH} + \text{B} \overset{\text{M}}{\rightleftharpoons} \text{R–O}^- + \text{BH}^+ \qquad (3)$$

where B is a base that can be either a water molecule or a stronger base and M denotes a metal ion, if present, or otherwise simply a water molecule. The energetics of eq 3 (in solution) can be described by Figure 8a, which shows the influence of some prototypes for B and M on the reaction free energy. The approximate numerical values in Figure 8a are calculated from observed pK values in solution. If we think of Figure 8a as defining a free energy surface for the solution reaction (3), it is interesting to examine to what extent this picture is reflected by enzymatic reactions of the same type. In Figure 8b a number of enzymes with well-characterized reaction mechanisms are "plotted" according to their catalytic machinery for handling eq 3. Although it is clear that the actual free energy values of Figure 8a cannot apply strictly to Figure 8b, e.g., because of different dielectric properties of the environments, it is suggestive that the "high-energy" region appears to be avoided in Figure 8b. This supports the notion that the "choices" of metals and bases in enzymes are in fact correlated with each other. The types of general-base catalysts represented by a carboxylate ion and an imidazole ring in Figure 8 can also, tentatively, be classified in terms of the two different types of charge redistributions associated with the proton-transfer reaction (eq 3). That is, when a carboxylate ion acts as a general base, one unit of negative charge is simply "moved" from the base to the nucleophile ([–0] → [0–]). With an imidazole ring as the proton acceptor, on the other hand, an ion pair is created by the reaction ([0 0] → [+–]). In the latter case the ion pair is often "prestabilized", without a metal, by the charge distribution of the active site (e.g., by an Asp–His pair as in the serine proteases). It would appear that such a prestabilization of the resulting configuration (relative to the reactant state) is easier to achieve in the [0 0] – [+–] case, since the character of the charge distribution changes more drastically. With this simple type of charge redistribution picture in mind, one could perhaps attempt to examine more distantly related

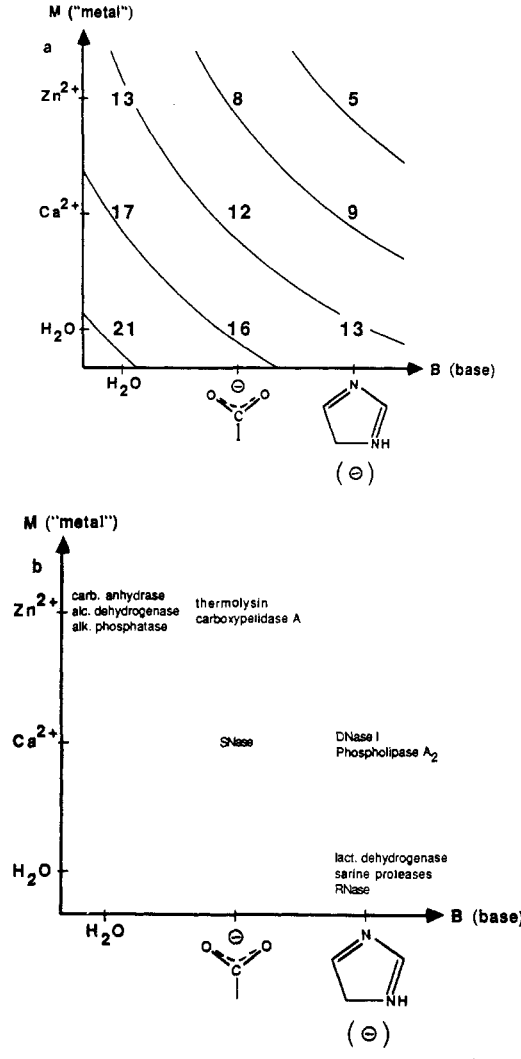

Figure 8. (a) Diagram showing the effects of metal ion and general-base catalysts on the reaction of eq 3. The abscissa denotes increasing general-base strength, represented by a water molecule, a carboxylate ion, and an imidazole ring. The ordinate represents increasing metal ion electrophilicity, where a water molecule denotes the case where no metal is present. The energy values, ΔG_{ij}, correspond to the proton-transfer reaction $(M^{2+}{}_i)H_2O + B_j \rightleftharpoons (M^{2+}{}_i)OH^- + BH^+{}_j$ where each entry is obtained from $\Delta G_{ij} = -2.3RT(pK_j - pK_i)$. For example, in the case of a metalloenzyme using Ca^{2+} and glutamate, respectively, as M and B, i denotes $Ca^{2+}(H_2O)$ and j denotes (Glu)-COOH (the pK_a's for metal bound water are taken from ref 12). (b) The figure shows a number of different enzymes that catalyze reactions involving a proton-transfer step like eq 3, plotted according to their use of metal ion and general-base catalysis (SNase, DNase I, and RNase denote staphylococcal nuclease, deoxyribonuclease I, and ribonucleases [e.g., A and T_1], respectively).

enzymatic proton-transfer mechanisms. For instance, the proton-transfer step in lysozyme would correspond (see reference 27) to the [0 0] → [+–] case with prestablization by Asp 52.

The discussion in the preceding paragraph should be regarded as a somewhat speculative attempt to rationalize the relations between the roles of metal and general-base catalysis in enzymes only as far as proton transfer is concerned. In reality there are, of course, several additional factors that determine the efficiency of a particular catalytic configuration, notably the nature of the rate-limiting transition state (as our calculations on SNase show)

(27) Warshel, A. *Proc. Natl. Acad. Sci. U.S.A.* **1978**, *75*, 5250–5254.

(28) If a very electrophilic metal already binds the hydroxide ion in Ψ_1 (i.e., the OH^- is a ligand of the metal), then it is important to also consider the alternative mechanism, where a water molecule in the next solvation shell provides the reactive OH^- nucleophile. However, in this case we also expect to find an increase in ΔG^* since the metal would not be so effective in stabilizing the hydroxide formed in the proton transfer step.

and the requirement for proper binding of substrates. It should also be realized that the active-site microenvironment, as a whole, determines the catalytic properties of a given enzyme rather than just one or two catalytic groups. Future calculations on the enzymatic reactions discussed above can hopefully reveal some of the rationales behind the particular choices of metal ions, but it seems likely that the general free energy relationships leading to optimization for Ca^{2+} in SNase will be relevant also in other cases.

Acknowledgment. J.Å. gratefully acknowledges support from the Swedish Natural Science Research Council. Support from the office of Naval Research (Contact N00014-87-K0507) is also acknowledged.

Ab Initio Computational Study of Methano- and Ethano-Bridged Derivatives of Oxyallyl

Andrew S. Ichimura,[1] Paul M. Lahti,*[,1] and Albert R. Matlin[2]

Contribution from the Department of Chemistry, University of Massachusetts, Amherst, Massachusetts 01003, and Department of Chemistry, Oberlin College, Oberlin, Ohio 44074. *Received June 30, 1989*

Abstract: Ab initio SCF-CI computations on methano-bridged oxyallyl (OA) (**3**) and ethano-bridged OA (**4**) indicate that the OA's are ground-state singlet species, with strong C=O bonds and pronounced diradicaloid character in the CI wave functions. The computational excited $^3B_2$ π-π^* states of **3** and **4** are ~4-7 kcal/mol higher in energy than the $^1A_1$ ground-state diradicaloids. The bicyclobutanone analogue of **3S** (**5**) is predicted to be substantially lower in energy than any of the diradicaloid forms, but the bicyclopentanone analogue of **4S** (**6**) is somewhat higher in energy than **4S**. Experimental observation of the triplet manifold of these OA derivatives is likely to be rendered quite difficult by their small singlet-triplet gaps and the thermodynamic accessibility of the bicyclic analogues. Qualitative molecular orbital considerations suggest that electron-rich olefins might be trapped by a nonconcerted mechanism, in accord with recent experimental results.

Oxyallyl (OA, **1**) and related molecules have been discussed as reactive intermediates or transition states in a number of reactions,[3-8] despite an apparent dearth of clear experimental evidence for their direct observation. In such a situation where experiment has been less than clear-cut, computational chemical methods can be useful to clarify the problem. Semiempirical and ab initio computational studies have been carried out on OA's, with the most sophisticated published study to date predicting a modest preference for a ground-state (GS) π,π^* $^3B_2$ state[8] in the parent system **1**, despite the possible stabilizing influence on the $^1A_1$ state of closed-shell zwitterionic resonance structure **2**. The computed triplet-singlet (T-S) gap was small enough to leave to question as to whether higher levels of theory might reverse the favoring of a high-spin GS for OA. In addition, consideration of various OA's leads one to query the effects of substitution on the OA state energy ordering, lest by apparently innocuous changes in the OA system one might substantially alter its nature.

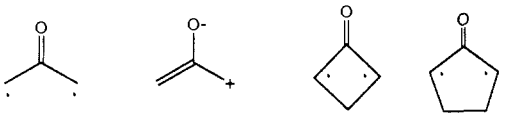

1 **2** **3** **4**

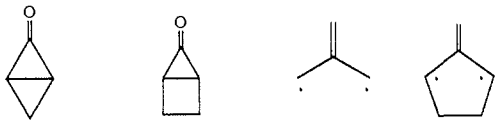

5 **6** **7** **8**

Two such likely OA derivatives of interest for experimental study are methano-bridged OA (**3**) and ethano-bridged OA (**4**) and their ring-closed bicyclic forms **5** and **6**. Similar derivatives have been employed in the study of trimethylenemethane[9,10] (TMM, **7**), where general system **8** has been much studied. Since bridging of **7** to **8** is accompanied by strain incorporation, cyclization is less favorable than for the unbridged system, making it is easier to study the diradical. Use of methano and ethano bridging in the OA system could, in principle, lead to a similar favoring of ring-opened forms **3** and **4**. The following computational study is aimed at elucidating the GS multiplicity of **3** and **4**, the approximate stability of the ring-opened vs the bicyclic forms, and the general electronic nature of the bridged OA's. Given recent theoretical[11,12] and experimental[13,14] interest in un-

(1) University of Massachusetts.
(2) Oberlin College.
(3) Turro, N. J. *Accts. Chem. Res.* **1969**, *2*, 25.
(4) Liberles, A.; Greenberg, A.; Lesk, A. *J. Am. Chem. Soc.* **1972**, *94*, 8685. Liberles, A.; Kang, S.; Greenberg, A. *J. Org. Chem.* **1973**, *38*, 1922.
(5) Chan, T.; Ong, B. S. *J. Org. Chem.* **1978**, *43*, 2994; *Tetrahedron* **1980**, *36*, 2269.
(6) Schaad, L. J.; Hess, B. A.; Zahradnik, R. *J. Org. Chem.* **1981**, *46*, 1909.
(7) Hoffmann, R. *J. Am. Chem. Soc.* **1968**, *90*, 1475.
(8) Osamura, Y.; Borden, W. T.; Morokuma, K. *J. Am. Chem. Soc.* **1984**, *106*, 5112.
(9) For reviews of the chemistry of ethano-bridged TMM's cf. the following: Berson, J. A. *Acc. Chem. Res.* **1978**, *11*, 446. Berson, J. A. In *Diradicals*; Borden, W. T., Ed.; Wiley: New York, 1982.
(10) The results of efforts to observe methano-bridged TMM's are summarized in the following: Lahti, P. M.; Berson, J. A. *J. Am. Chem. Soc.* **1981**, *103*, 7011. Lahti, P. M. Ph.D. Thesis, Yale University, New Haven, CT, 1985.
(11) Lahti, P. M.; Ichimura, A. S.; Berson, J. A. *J. Org. Chem.* **1989**, *54*, 958. Cf. also literature references to some earlier computational and theoretical work by various workers on the non-Kekulē molecules discussed in this paper.
(12) Du. P.; Hrovat, D. A.; Borden, W. T. *J. Am. Chem. Soc.* **1986**, *108*, 8086.
(13) Stone, K. J.; Greenberg, M. M.; Goodman, J. L.; Peters, K. S.; Berson, J. A. *J. Am. Chem. Soc.* **1986**, *108*, 8088.
(14) Zilm, K. W.; Merrill, R. A.; Greenberg, M. M.; Berson, J. A. *J. Am. Chem. Soc.* **1987**, *109*, 1567.

0002-7863/90/1512-2868$02.50/0